This is the peer reviewed version of the following article: Pawar, Harshavardhan V., Boateng, Joshua S., Ayensu, Isaac and Tetteh, John (2014) *Multifunctional medicated lyophilised wafer dressing for effective chronic wound healing*. Journal of Pharmaceutical Sciences, 103 (6). pp. 1720-1733. doi:10.1002/jps.23968, which has been published in final form at http://dx.doi.org/10.1002/jps.23968.

Multi functional medicated lyophilised wafer dressing for effective chronic wound healing.

Harshavardhan V. Pawar[1*], Joshua S. Boateng[1*#], Isaac Ayensu[1, 2], John Tetteh[1]

[1]Department of Pharmaceutical, Chemical & Environmental Sciences, Faculty of Engineering and Science, University of Greenwich at Medway, Central Avenue, Chatham Maritime, ME4 4TB, Kent, UK.

[2] Department of Pharmaceutical Chemistry, Faculty of Pharmacy and Pharmaceutical Sciences, Kwame Nkrumah University of Science and Technology, Kumasi, Ghana

* Harshavardhan Pawar and Joshua Boateng are joint first authors.

[#] Corresponding author: (Joshua S Boateng)

Tel: + 44 (0) 208 331 8980, Fax: +44 (0) 208 331 9805

E-mail: J.S.Boateng@gre.ac.uk; joshboat40@gmail.com

Abstract

Wafers combining weight ratios of Polyox with carrageenan (75/25) or sodium alginate (50/50) containing streptomycin and diclofenac were prepared to improve chronic wound healing. Gels were freeze dried using a lyophilisation cycle incorporating an annealing step. Wafers were characterised for morphology, mechanical and *in vitro* functional (swelling, adhesion, drug release in the presence of simulated wound fluid) characteristics. Both blank and drug loaded wafers were soft, flexible, elegant in appearance and non-brittle in nature. Annealing helped to improve porous nature of wafers but was affected by addition of drugs. Mechanical characterisation demonstrated that the wafers were strong enough to withstand normal stresses but also flexible to prevent damage to newly formed skin tissue. Differences in swelling, adhesion and drug release characteristics could be attributed to differences in pore size and sodium sulphate formed due to salt forms of the two drugs. Blank wafers showed relatively higher swelling and adhesion than drug loaded wafers with the latter showing controlled release of streptomycin and diclofenac. The optimised dressing has the potential to reduce bacterial infection and can also help to reduce swelling and pain associated with injury due to the anti-inflammatory action of diclofenac and help to achieve more rapid wound healing.

Keywords: Anti-infectives, Anti-inflammatory, Dressing, Freeze drying/lyophilisation, FTIR, *In vitro* drug release, Adhesion, Swelling, Wafers, Wound healing, X-ray diffractometry,

List of abbreviations

ATR-attenuated total reflectance;

BLK-blank;

BSA-bovine serum albumin;

CAR-carrageenan

DLF-diclofenac sodium;

DL-drug loaded;

DSC-differential scanning calorimetry;

FTIR-Fourier transform infrared;

POL-Polyox^{TM};

SA-sodium alginate,

SEM-scanning electron microscopy;

STP-streptomycin sulphate;

SWF-simulated wound fluid;

TA – texture Analysis;

XRD-X-ray diffraction;

WOA-work of adhesion

1 Introduction

According to the Wound Healing Society (WHS), a wound is the consequence of disruption of normal anatomic structure and function. It usually describes the rupture or defect in skin or body tissue due to physical or thermal damage or a consequence of underlying physiological and medical conditions[1]. The wound healing process is a complex phenomenon and involves different phases such as haemostasis, inflammation, proliferation, remodelling and scar maturation which are discussed elsewhere[1-3]. Based on the nature of the repair process, wounds are classified as acute and chronic. Compared with acute wounds, chronic wounds represent a medical challenge due to various complicating factors including diabetes and malignancies, chronic systemic inflammation, persistent infection, destruction of neighbouring tissues, poor primary treatment and other patient related factors such as poor nutrition[4].

The management of chronic wounds places an enormous drain on healthcare resources; with some studies estimating the cost of wound care management to the UK National Health Service (NHS) to be about £1billion a year. In the UK, around 24,000 admissions a year involve patients with diabetic foot ulceration alone, thereby costing the NHS some £17million[5]. Winter's theory of wound healing introduced a new approach for achieving rapid wound healing by maintaining a moist environment around the wound[6]. This principle of moist wound healing formed the basis of increased demand for developing a new range of modern wound dressings that can absorb excess of exudate and allow the maintenance of adequate moisture at wound surfaces. Further, different types of wounds (e.g. acute, chronic, exuding and dry wound) also affect the choice of dressing and in fact, no single dressing fulfils all the requirements (ideal characteristics) suitable for the management of all wounds[1].

Wound exudate from acute wounds contains many endogenous substances which typically reflect the overall wound healing process. These include epithelial and fibroblast cells which have been shown to increase the rate and quality of wound healing[7]. On the other hand,

most chronic wound exudates are associated with bacteria, dead white cells in combination with high levels of inflammatory mediators and protein-digesting enzymes which can be unfavourable for the wound healing process[8]. In modern wound care practice, iodine, silver and broad spectrum germicidal agents such as neomycin, bacitracin, polymyxin, STP, gentamycin and/or combinations are used to control and treat bacterial infection in chronic wounds. Local delivery of these antibiotics in the form of dressings is more convenient over their systemic counterparts since they deliver a higher concentration of medication directly to the desired area and are less frequently implicated in causing bacterial resistance[9].

Polysaccharides, being naturally occurring biomolecules, are an obvious choice for application as potential wound management aids[10]. It has been previously demonstrated that the use of synthetic and natural polymers helps to improve the properties which makes them suitable for application in the biomedical field[11]. Pawar and co-authors prepared films from blends of synthetic and natural polymers for potential improvement in chronic wound healing[12]. However, highly exuding chronic wounds such as diabetic foot and venous ulcers limit the application of film dressings due to the high amount of exudate produced. Film dressings being poor at absorbing large volumes of exudate, allow the fluid to collect beneath the dressing, causing maceration at the wound site and therefore require frequent dressing changes which adversely affects patient compliance.

Lyophilised wafers are produced by freeze-drying polymer solutions and gels to yield solid porous structures that can easily be applied to exuding wound surfaces[13]. It is anticipated that a lyophilised polymer matrix would preserve the size, shape and form of contained compounds unlike a conventional gel suspension, where crystal ripening, agglomeration and polymorphic changes may occur[14]. Their physical architecture resembles those of foam dressings which are made of porous polyurethane. Drug stability is better in a lyophilised dosage form compared to a semi-solid hydrogel based formulation[15]. Lyophilized wafers provide a potential

means of delivering pharmacological agents to wound surfaces to aid healing[16]. They have the ability to incorporate soluble and insoluble antimicrobial compounds greater than their minimum bactericidal concentration for antibacterial activity against pathogenic bacteria[17]. Wafers have the capacity to absorb large amounts of exudate due to their porous nature whilst maintaining a moist environment without damaging newly formed tissue. Wafers also offer high drug loading capacity compared to solvent cast films[18].

This study involves preparation and functional characterisation of lyophilised wafers of Polyox (POL) in combination with carrageenan (CAR) or sodium alginate (SA) loaded with streptomycin (antibacterial) and diclofenac (anti-inflammatory) to target infection and the inflammatory phase of wound healing. The prepared wafers were characterised by scanning electron microscopy (SEM), X-ray diffraction (XRD), Fourier transform infrared spectroscopy (FTIR) and mechanical properties using texture analyser. The optimised wafers were further evaluated for functional bio-analytical properties such as swelling, adhesion and drug release properties.

2 Experimental

2.1 Materials

Polyethylene oxide (Polyox™ WSR 301 ≈4000 kDa) was obtained as a gift from Colorcon Ltd (Dartford, UK), κ-carrageenan (Gelcarin GP 812 NF) was obtained from IMCD Ltd (Sutton, UK), sodium hexane sulphonate, sodium phosphate tribasic, dodecahydrate (>98%), bovine serum albumin (BSA), diclofenac sodium (DLF) and streptomycin sulphate (STP) were all purchased from Sigma Aldrich, (Gillingham, UK). Sodium alginate (SA), acetonitrile (HPLC grade), glycerol (GLY), tris (hydroxy) aminomethane, calcium chloride dihydrate, ethanol (laboratory grade), orthophosphoric acid (analytical grade) were all purchased from Fisher Scientific (Leicestershire, UK).

2.2 Preparation of POL-CAR and POL-SA gels

Blank (BLK) polymeric gels (1% w/w) of polyox (POL) and carrageenan (CAR) and POL and sodium alginate (SA) were prepared according to previously reported methods[12,19]. In brief, blends of POL with CAR and POL with SA (weight ratio of 75/25 and 50/50) respectively yielding 1% w/w of total polymer weight, were prepared by stirring on a magnetic stirrer at 70°C to form a uniform gel. The drug loaded (DL) gels were prepared by the addition of an ethanolic solution of DLF to the polymeric gel (as described above) at 70°C to obtain a final DLF concentration of 10 and 25% w/w. respectively for POL-SA and POL-CAR gels. The gel was subsequently cooled to 40°C with constant stirring and an aqueous solution of STP was subsequently added to achieve a final STP concentration of 25 and 30% w/w respectively for POL-SA and POL-CAR gels. The amounts of the polymers and drugs used for the preparation of gels are summarised in Table 1.

2.3 Freeze drying cycle development

Prior to lyophilisation, preliminary DSC studies on the BLK (POL-CAR and POL-SA) gels were carried out. A differential scanning calorimeter DSC-1 (Mettler Toledo Ltd, Leicester, UK), calibrated with indium (at 10°C/min) was used to analyse the thermal events in the gels to determine a more suitable lyophilisation cycle. The blank (BLK) gels were cooled in 40 µl aluminium pans (ME-00026763, Metler Toledo) from 25 to -60°C at a rate of 10°C/min. They were then re-heated back to 25 °C at 20 °C/min and the cycle repeated three times. Based on thermal events observed during the heating cycles, an annealing temperature of -25°C was chosen. The samples were then cooled to -60°C, warmed to -25°C, held at that temperature for 10 min, cooled back to -60°C and then warmed through to 25°C at 20°C/min.

2.4 Wafer preparation

The freeze-dried wafers were prepared by freeze-drying (10 gm) of each homogeneous gel in 6 well moulds (diameter 35 mm) (Corning® CellBIND® Sigma Aldrich, Gillingham, UK) in a Virtis Advantage XL 70 freeze dryer (Biopharma Process Systems, Winchester, UK) using an automated novel lyophilisation cycle (Figure 1). This involved initially cooling and freezing including annealing step for samples from room temperature to -5°C and then -50°C over a period of 10 h (at 200 mTorr). An annealing step at -25°C for 2 h was applied and its effect on the drug loaded formulation investigated. The frozen samples were then heated in a series of thermal ramps to -25°C under vacuum (20-50 mTorr) over a 24 h period. Secondary drying of the wafers was carried out at 20°C (10 mTorr) for 7 h. The wafers were designated as 'An' (annealed) or 'NAn' (non-annealed).

2.5 Scanning electron microscopy (SEM)

Surface morphology of the lyophilised wafers was analysed by a Hitachi SU 8030, (Hitachi High-Technologies, Germany) scanning electron microscope at low accelerating voltage (1 kV). Wafers were cut into thin slices and mounted on aluminium stubs (1 inch diameter) with 'Agar Scientific G3347N' double sided adhesive carbon tape. Images of the wafers were acquired at a working distance of 15.0 mm at magnifications of 500-1500.

2.6 X-ray diffraction (XRD)

XRD analyses of the prepared wafers were performed using a D8 Advantage X-Ray diffractometer (Bruker AXS GmbH, Karlsure, Germany). The lyophilised wafers were compressed to a width size of 0.5 mm using a clean pair of compression glasses and mounted on the sample holder. The transmission diffractograms were acquired using DIFFRAC plus XRD Commander over a start to end diffraction angle of 2θ from 5° to 45°, step size of 0.02 and a

scan speed of 0.4 sec. X-ray patterns of the wafers and starting materials were obtained with DIFFRAC plus (Bruker Coventry, UK) having an XRD commander programme. A Goebbel mirror was used as monochromator which produced a focused monochromatic $CuK_{\alpha 1\&2}$ primary beam (λ=1.54184 Ǻ) with an exit slit of 0.6 mm. The detector used for performing the experiment was Lynx Eye. The operating condition during the experiment was 40 kV and 40 mA.

2.7 Differential scanning calorimetry (DSC)

DSC analysis of the POL-CAR and POL-SA (BLK and DL) wafers and starting materials (CAR, SA, DLF and STP) was undertaken on a DSC1 Mettler Toledo instrument (Leicester, UK) calibrated with indium (based on heating range). Wafers were cut into small pieces and 3-5 mg of sample was placed into 40µl aluminium pans with lids (Mettler Toledo, Leicester, UK) and sealed using crucible sealing press (Metler Toledo Leicester, UK). An empty aluminium pan sealed with lid was used as reference. A *STAR*^{e} software program was used to run the samples by initially cooling from 25°C to -50°C and then heated from (-50°C to 350°C) at the rate of 10°C/min under constant purge of nitrogen (100 ml/min) to evaluate the thermal behaviour of the polymers and drugs present in the wafers.

2.8 Attenuated total reflectance Fourier transform infrared spectroscopy (ATR-FTIR)

A FTIR spectrophotometer was used in combination with (Thermo Nicolet, Thermoscientific, UK), ZnSe attenuated total reflectance (ATR) accessory to characterise the wafers. The FTIR was equipped with potassium bromide (KBr) beam splitter and MCT detector. The wafers were placed on ZnSe ATR crystal (45°) and maximum pressure was applied by using a pressure clamp accessory to allow for intimate contact of the wafers with the ATR crystal. Similarly, the pure starting materials (POL, CAR, SA, STP and DLF) were analysed as controls.

Spectra were recorded at 4 cm^{-1} resolution within a range of 650-4000 cm^{-1} using OMNIC® software. True absorbance of each sample was obtained by background subtracting spectral information for the ATR crystal.

2.9 Mechanical strength ('hardness')

The mechanical properties (resistance to deformation and ease of recovery) of the freeze-dried wafers were investigated by compressing on a Texture Analyser (TA) (Stable Microsystems Ltd., Surrey, UK) equipped with 5 kg load cell and *Texture Exponent-32*® software program[18]. Wafers were compressed using a 6 mm (P/6) cylindrical stainless steel probe (Stable Microsystems Ltd., Surrey, UK) in compression mode. The effects of compression speed (0.1-3.0 mm/sec) and depth of penetration (0.2-3.0 mm) on different wafers were evaluated. The 'hardness' (resistance to deformation) of the wafers were evaluated by compressing the sample at three different locations to a depth of 2 mm at a speed of 1 mm/sec using a trigger force of 0.001N and withdrawn till it lost complete contact with the wafer. Five wafers of each formulation [POL-CAR and POL-SA (NAn, An, and DL-An)] were compressed to determine the reproducibility in the response of the wafers to deformation by compression.

2.10 Swelling studies

Four different annealed (An) wafers POL-CAR-BLK-An, POL-CAR-DL-An, POL-SA-BLK-An, and POL-SA-DL-An were used for the swelling studies. The swelling studies were carried out as described previously[19]. In brief, the wafers were immersed in simulated wound fluid (SWF) containing (2% bovine serum albumin, 0.02 M calcium chloride, 0.4 M sodium chloride, 0.08 M tris (hydroxyl) aminomethane in deionised water, pH 7.5) at room temperature[20]. The change in weight of the hydrated wafers was determined every 15 min up to 120 min. The hydrated wafers were carefully blotted with tissue paper to remove excess SWF on

the surface and then weighed immediately on an electronic balance (European Instruments, UK). The effect of polymer and drugs on swelling performance was evaluated for the four formulations. Percentage swelling index *Is* (%) was calculated using the equation 1[19]. Where, W_d is dry weight of polymeric wafers and W_s denotes weight of the hydrated swollen wafer.

$$Is = \frac{Ws - Wd}{Wd} \times 100 \qquad \text{Equation 1}$$

2.11 In vitro adhesion studies

Adhesive measurements were performed on the wafers using a TA.HD *plus* Texture Analyser (Stable Micro Systems, Surrey, UK) fitted with a 5 kg load cell. The wafer (n = 4) was attached to an adhesive probe (75 mm diameter) using double sided adhesive tape. The surface of a 6.67 % w/v gelatine solution, allowed to set as a solid gel in a Petri dish (86 mm diameter), was equilibrated with 0.5 ml 2% w/w BSA containing SWF or 5% w/w BSA containing SWF to mimic a wound surface with thin and viscous exudate respectively. The probe, lined with wafer was set to approach the model wound surface with the following pre-set conditions: pre-test speed 0.5 mm/s; test speed 0.5 mm/s; post-test speed 1.0 mm/s; applied force 1 N; contact time 60.0 s; trigger type auto; trigger force 0.05 N and return distance of 10.0 mm. The adhesive characteristics were determined by the maximum force (stickiness) required to detach the wafer from the model wound surface, total work of adhesion (WOA) was represented by the area under the force versus distance curve, whilst cohesiveness was defined as the distance travelled by wafer till detached and calculated using the *Texture Exponent 32*® software.

2.12 In vitro drug dissolution studies

Drug assayed contents of STP and DLF within the wafers were determined before performing the drug dissolution studies. These were measured by cutting wafers from different sections of the wafers into small pieces, accurately weighed to 4 mg and hydrated in 10 ml of

distilled water at 37°C with stirring and left overnight to completely dissolve. The concentration of STP and DLF in distilled water was assayed by HPLC as described in *2.13*. *In vitro* drug dissolution studies were performed with a Franz diffusion cell across a wire mesh using SWF (without BSA) at pH 7.5 as dissolution media in the receptor compartment. The pH 7.5 was chosen in order to represent the natural chronic wound environment which has been reported in range of 7.15–8.90 [21]. The SWF was prepared without BSA to avoid blocking the HPLC column. The DL wafers (POL-CAR-DL and POL-SA-DL) containing STP and DLF was placed on the wire mesh. The donor and receiver compartments were kept in intimate contact by wrapping Parafilm® at the junction between both compartments. POL-CAR-BLK and POL-SA-BLK were used as control. The temperature of the diffusion cell was maintained at 37±0.5°C by a circulating water jacket. The dissolution medium was constantly stirred throughout the experiments using magnetic beads on a magnetic stirrer. 1.0 ml aliquots of dissolution media were withdrawn at predetermined time intervals and analysed by HPLC and replaced with the same amount of SWF to maintain a constant volume throughout. The percentage cumulative release of STP and DLF from the wafers was calculated, taking into consideration the dilution due to the 1.0 ml aliquots that were discarded and replaced with fresh dissolution medium. The calculated values were plotted against time.

2.13 HPLC analysis

This was performed using an Agilent 1200 HPLC equipped with an auto sampler (Agilent Technologies, Cheshire, UK,) and a Chemstation® software program. The column used was a Hichrome (150 x 4.6 mm, 5µm) (Hichrome ltd; Berkshire, UK). The mobile phase consisted of phosphate buffer (pH 5.5) and acetonitrile in the ratio of 85:15 (v/v) for STP and deionised water and acetonitrile in the ratio of 40:60 (v/v) for DLF. The buffer was prepared by mixing 20mM of sodium hexane sulphonate and 25mM of tribasic sodium phosphate in distilled

water and pH adjusted to 5.5 using ortho-phosphoric acid. The flow rate of the mobile phase was maintained at 1.0 ml/min and detector wavelengths for STP and DLF were set at 195 nm and 284 nm respectively. 20 µl volumes were injected during each run. Standards from 5-500µg/ml were used to plot calibration curves for STP and DLF (r^2> 0.99).

3 Results

3.1 Freeze drying cycle development with annealing step

Table 2 shows the DSC thermal transition profiles of gels evaluated from -60°C to 25°C which informed the freezing [annealing (An)/non-annealing (NAn)] stages during the development of the freeze drying cycle of the prepared polymeric gels. Glass-transition (Tg) temperature of -54.5°C and -56.9°C was observed for the POL-CAR gel and POL-SA gels respectively. The eutectic melts for both gels were observed between -8°C to -13°C and ice melts were observed between an onset of -1.0°C and endset of (6-11°C) which is associated with melting of ice in the interstitial spaces of the frozen cake. Table 2 also shows the transitions during the heating stage of the POL-CAR-An and POL-SA-An gels, where no glass transition but rather the eutectic melt [-10.5°C (POL-CAR-An gel), -9.5°C (POL-SA-An gel)] and ice melt [2.0°C (POL-CAR-An gel), 2.6°C (POL-SA-An gel)], were observed. The effectiveness of the annealing process was evidenced by the disappearance of the glass transition in the heating cycle.

3.2 Formulation development and optimisation

The different wafers (POL-CAR-BLK, POL-CAR-DL, POL-SA-BLK, and POL-SA-DL) both annealed and non-annealed (An and NAn respectively) were visually examined for acceptable lyophilisation behaviour and physical elegance of the resulting product. All wafers prepared from the blending of POL-CAR and POL-SA were of uniform mass, texture and

thickness, soft and flexible especially POL-SA wafers which were softer and more pliable in nature compared to POL-CAR wafers.

3.3 Scanning electron microscopy

SEM images of POL-CAR-BLK (NAn and An), POL-CAR-DL-An, POL-SA-BLK (NAn and An) and POL-SA-DL-An wafers are shown in figure 2. POL-CAR-BLK-An and POL-SA-BLK-An wafers formed a porous interconnecting network of polymeric strands having circular shaped pores after annealing. POL-CAR-BLK-NAn showed smaller pores with a leafy structure whilst POL-SA-BLK-NAn wafers showed elongated sponge-like strands with a less porous structure. POL-CAR-BLK-An wafers formed a sponge-like network whilst POL-SA-BLK-An wafers formed a less porous structure. Overall, the SEM images showed a tangible effect of annealing on the pore distribution of the wafers.

The SEM images of POL-CAR-DL-An and POL-SA-DL-An wafers showed significant differences in surface topography. The POL-CAR-DL-An wafer at high drug loading (25% w/w DLF and 30% w/w STP based on total polymer weight) showed the least porosity as the surface texture appeared as leafy strands with irregular pores while the POL-SA-DL-An wafer (at 10% w/w DLF and 25% w/w STP based on total polymer weight) showed a more porous texture with uniform pore size distribution.

3.4 Mechanical properties of wafers

Table 3 shows the effect of speed and depth of probe penetration on the 'hardness' (resistance to compression) of POL-CAR-BLK and POL-SA-BLK (NAn and An) in addition to POL-CAR-DL-An and POL-SA-DL-An wafers. The results show slight increases in the resistance to compressive deformation with increasing test speed. POL-CAR-BLK-NAn wafers showed high resistance to compressive forces at all speeds (0.2 - 3.0 mm) but was decreased for

the POL-CAR-BLK-An wafers. There were slight differences in the 'hardness' between the POL-CAR-BLK-An and POL-CAR-DL-An as well as between POL-SA-BLK-An and POL-SA-DL-An wafers. Generally, the POL-CAR-An wafers (both BLK and DL) were stronger ('harder') than the corresponding POL-SA-An (BLK and DL) wafers. In the case of the POL-SA formulations, the difference between the BLK and DL wafers were less and also showed an effect opposite to that for POL-CAR. In other words, whereas the 'hardness' of the POL-CAR-BLK-An (0.96 ± 0.1) was higher than POL-CAR-DL-An (0.74 ± 0.3), the value for POL-SA-BLK-An (0.44 ± 0.1) was lower than POL-SA-DL-An (0.55 ± 0.1).

When wafers were compressed to a greater penetration depth, the peak force required to deform the wafers increased due to the reduction in porosity of wafers at greater depths of compression and more intimate contact of the polymer chains. It was observed that a higher force was required for the probe to penetrate (2 mm) for all the wafers with increasing speed (Table 3). This may be due to the arrangement of the polymer network which resists penetration and requires a higher force with increased speed of compression. The POL-CAR (An and NAn) wafers showed significantly higher 'hardness' ($p < 0.001$) when compared with the POL-SA (An and NAn) wafers. This suggests that POL-CAR wafers showed a more rigid polymeric network than the POL-SA wafers and these results support the SEM observations.

3.5 X-ray diffraction (XRD)

Figure 3 shows XRD transmission diffractograms of POL, SA, CAR, DLF and STP. Pure POL was semi-crystalline in nature which showed sharp peaks at 14.62°, 15.05°, 19.11°, 23.22°, 26.23° and 26.91° whereas CAR indicated an amorphous nature with the presence of peak at 28.39°, and 40.58° which may be attributed to inorganic salt impurities, mainly potassium chloride (KCl)[22]. STP and SA were amorphous whilst DLF was highly crystalline in nature. XRD diffractograms of annealed wafers prepared from POL-CAR and POL-SA (BLK and DL)

are also shown in figure 3. POL-CAR-BLK-An and POL-SA-BLK-An wafers showed decreased intensities at 19.11°, 23.22° which indicates that the crystallinity of POL was reduced in the presence of CAR and SA. Further, POL-SA-BLK-An wafers showed decreased intensities due to the relatively higher ratio of SA compared to CAR. All the drug loaded wafers did not show distinct peaks of DLF and STP, however, there was a peak observed at 31.73° which may be associated with the formation of sodium sulphate associated with the DLF and STP.

3.6 Differential scanning calorimetry (DSC)

Figure 4 shows the DSC thermograms for pure polymers, pure drugs and their corresponding wafers. STP showed a broad endothermic peak at 152.7°C which undergoes recrystallization and then eventually melts. This may be associated with the presence of basic guanido moieties and relatively weakly basic methylamino functional groups which are responsible for two melt peaks and needs further investigation. SA showed a glass transition peak at 60.3°C with subsequent endothermic peaks at 152.7°C, whereas CAR showed an endothermic peak at 148.8°C which consequently decomposed at 192.6°C with a sharp exothermic peak. DLF showed melting peaks at 293.9°C in addition to immediate decomposition. POL showed an endothermic peak at 70.2°C with an exothermic peak at 177.2°C which could be attributed to the recrystallization from the melt. DSC curves of all POL-CAR and POL-SA (BLK and DL) An wafers showed a reduction in the intensity of the POL melting peak (59 - 61°C) due to the molecular chain of CAR and SA which has a significant effect on the overall chain mobility in the mixture and retards the rate of crystal growth of POL[12].

POL-CAR-BLK-An wafers further showed an exothermic peak at 130°C due to the POL but this was absent in the POL-CAR-DL-An wafers due to the drug-polymer interaction. POL-CAR (BLK-An and DL-An) wafers showed endothermic peaks between (162 - 164°C) which may be associated with CAR. POL-CAR (BLK-An and DL-An) wafers showed exothermic

peaks at 212.3°C and 270.4°C respectively which may be due to the interactions between the polymer and drug. POL-SA (BLK-An and DL-An) wafers showed an endothermic peak at 135.3°C and 139.9°C and exothermic peak 238.7°C and 242.2°C possibly due to the effect of added SA. Wafers showed hydrogen bonding interaction between the polymer blends of POL-SA and POL-CAR which confirms the compatibility of these polymers. Both POL-CAR-DL-An and POL-SA-DL-An wafers did not show any peaks for DLF and STP which suggests the molecular dispersion of the drugs within the wafer matrix.

3.7 Attenuated total reflectance Fourier transform infrared spectroscopy (ATR-FTIR)

Figure 5 shows the ATR-FTIR spectra of POL-CAR and POL-SA (BLK-An, and DL-An) wafers. The spectra show the respective absorption peaks of POL at 1100cm^{-1} due to C-O-C asymmetric stretching. An absorption band at 2885cm^{-1} was also attributed to CH symmetric stretching vibration in POL, while absorption bands at 1465cm^{-1}, 1242cm^{-1}, 1278cm^{-1} and 958cm^{-1} were associated with CH_2 scissoring, asymmetric twisting and wagging respectively. CAR showed an absorption peak at 1232cm^{-1} due to the presence of sulphate ester moiety. The peaks at 924cm^{-1}, 844cm^{-1}, 890cm^{-1} and 1155cm^{-1} were respectively assigned to 3, 6 anhydrogalactose residue, galactose 4-sulphate, C-H stretching of β-galactopyranosyl residue and C-O stretching of pyranose ring of the CAR. In the FTIR spectrum of SA, C-O stretching of uronic acid, C-C, C-O stretching and C-OH deformation vibrations were observed at 929cm^{-1}, 1024cm^{-1}, 1084cm^{-1}, 1400cm^{-1} respectively. DLF showed the characteristic peak at 1402cm^{-1}, 1573cm^{-1} which is due to the O-C-O symmetric and asymmetric stretching, whilst the observed peaks at 1556cm^{-1}, 1602cm^{-1}, 1585cm^{-1} are associated with ring stretching. Peaks at 1469cm^{-1} and 1450cm^{-1} were due to C-N stretching. The same stretching band of C-N at 1458cm^{-1} was observed for STP. Primary NH_2, O-H and C-O-C stretching at 3365cm^{-1}, 3201cm^{-1} and 1035cm^{-1} respectively was observed for STP.

Monitoring the band shift at 1100cm^{-1} C-O-C stretching for the BLK and DL POL-CAR and POL-SA wafers showed hydrogen bonding or complexation between the POL and both CAR and SA. Intermolecular interaction between the POL with CAR or SA was responsible for the increased physical stability of the prepared wafers. The DL wafers did not show any characteristic peaks of DLF due to the homogeneous mixing into the POL-CAR and POL-SA polymeric matrix. However, the presence of C=N and N-H stretching band at 1618cm^{-1}-1654cm^{-1} confirmed the presence of STP in all the POL-CAR (DL) wafers.

3.8 Swelling studies

Figure 6 shows the change in swelling capacity (%) of the wafers with time. The difference in the hydration capacity of the optimised POL-CAR-BLK-An wafer (3770 ± 283%) and POL-SA-BLK-An (1711 ± 46%) was statistically significant ($p = 0.0001$). The POL-CAR-BLK-An wafers showed high swelling capacity which was dramatically decreased in the POL-CAR-DL-An wafers (1450 ± 62%). This difference was also observed between the POL-SA-BLK-An and POL-SA-DL-An wafers even though the differences were only noticeable during the first 40 minutes. The POL-SA-DL-An wafer showed a maximum swelling capacity of only 1227 ± 134%.

POL-CAR-BLK-An showed higher swelling capacity than the POL-SA-BLK-An, which may be due to the use of different polymers in different ratios (75/25 and 50/50, respectively). In the initial 30 min, the swelling index of both DL wafers (POL-CAR-DL-An and POL-SA-DL-An) were the same which further decreased for POL-SA-DL-An but were consistently increasing for POL-CAR-DL-An.

3.9 Adhesion studies

Figure 7 shows the effect of two different concentrations of BSA (2% w/w and 5% w/w) representing thin (watery) and viscous exudate respectively, on adhesion properties of POL-CAR and POL-SA (BLK-An and DL-An) wafers. POL-CAR-BLK-An and POL-SA-BLK-An wafers showed similar (4.9 ± 1.3N and 4.7 ± 1.1N respectively) stickiness values in the presence of thin SWF (2% w/w BSA) whereas the stickiness was decreased in POL-CAR-DL-An and POL-SA-DL-An wafers. WOA and cohesiveness were higher in the POL-SA (BLK-An and DL-An) wafers which decreased for POL-CAR (BLK-An and DL-An) wafers. Both POL-CAR-BLK-An and POL-SA-BLK-An wafers showed high stickiness in the presence of viscous SWF (5% w/w BSA) which decreased for the POL-SA-DL-An and POL-CAR-DL-An wafers. It was observed that WOA decreased in descending order for POL-CAR-BLK-An, > POL-SA-BLK-An, > POL-SA-DL-An wafers. There was a significant difference ($p = 0.0010$) in stickiness and WOA between BLK-An and DL-An of both POL-CAR and POL-SA wafers. Overall, the POL-CAR-BLK-An wafers showed higher stickiness and WOA in the presence of viscous SWF (5% w/w BSA) whereas POL-CAR-DL-An wafers had higher stickiness and WOA in the presence of normal or thin SWF (2% w/w BSA). However, POL-SA-BLK-An and POL-SA-DL-An wafers showed higher stickiness and WOA in the presence of SWF (2% w/w BSA) compared to SWF (5% w/w BSA). In the presence of SWF (2% w/w BSA) POL-CAR (BLK-An and DL-An) had similar values while POL-SA (BLK-An and DL-An) showed significant differences in the cohesiveness ($p = 0.0200$).

3.10 In vitro drug release study

Figure 8 shows the dissolution profiles of STP and DLF from annealed POL-CAR-DL and POL-SA-DL wafers. The drug loading capacities for POL-CAR-DL-An wafers were 68.2 ± 1.1% (STP) and 90.2 ± 1.0% (DLF) whilst that for the POL-SA-DL-An wafers were 61.8 ±

18.4% (STP) and 93.9 ± 4.7% (DLF) (n = 3). The total cumulative percent of STP released in 72 h from the POL-CAR-DL-An wafer and POL-SA-DL-An wafers were 81.4 ± 3.8% and 79.6 ± 4.9%, respectively which was statistically significant (p = 0.0189), though both formulations exhibited a sustained (controlled) release of STP.

Model dependent methods based on mathematical functions were used to describe the dissolution profiles of STP and DLF released from the wafers. These included zero order, first order, Higuchi, Hixson-Crowell and Korsmeyer-Peppas models. Release parameters obtained from fitting experimental dissolution release data to the different kinetic equations have been summarised in Table 3. The slope (n) values ranged from 0.57 - 0.60 for STP and 0.60 - 0.84 for DLF in the case of wafers. The *in-vitro* release profiles of STP from the wafers could best be described by Korsmeyer-Peppas equation which showed the highest linearity (R^2 = 0.90 - 0.99) compared to the other equations (Table 4).

4. Discussion

The formulations with different ratios were selected based on preliminary studies undertaken with different hydrophilic polymers each at different combinations of concentrations with POL as part of the wider study[12]. The formulations in different w/w ratios, 75/25 for POL-CAR and 50/50 for POL-SA were selected on the basis of their ease of handling such as pouring and also forming clear transparent films that were better than POL (1% w/w) on its own (published in our previous article). In the future, we plan to compare the *in vivo* performance of the films and wafers and we wanted their polymer content to be comparable as this affects hydration, swelling, drug release and bioadhesion significantly.

According to Zivanovic and co-workers, formulations prepared from only synthetic polymers such as polyethylene oxide have relatively poor physical characteristics such as stickiness and high water solubility which limit their application[26]. Generally, formation of

specific intermolecular interactions through weak hydrogen bonding between two or more polymers is responsible for the observed behaviour of formulations prepared from aqueous gels comprising blends of polymers. The good film forming ability of CAR has been explored for the development of wound healing patches for the treatment of topical burn wounds[23]. A naturally occurring polymer (CAR) was added to POL to modify and improve the properties of the latter as well, due to its reported use for wound application. Hydrogel dressings containing polyvinyl alcohol, CAR and agar have been used in clinical trials on human patients which showed safety and efficacy of the dressing. Such dressings have been used in treatment of burns, non-healing diabetic ulcers, leprosy and other external wounds. This dressing is now being marketed in India under different brand names[24].

To avoid the formation of a metastable glass which will eventually crystallize and affect the stability of the formulations, samples were heated to above the measured glass transition temperature (but below the eutectic and/or ice melting temperature) of the mixture and temperature returned to the original freezing temperature. This allowed the glass to relax and crystallize during the freezing stage. It has previously been demonstrated that gels which are annealed between the glass transition and eutectic melt peaks improves the metastable state[14]. This leads to transformation of its structure towards a more relaxed state and is manifested by an improvement in functional characteristics such as hydration, adhesion and drug release properties of the formulations[14]. Based on the thermal events observed during the heating cycle, an annealing temperature of -25°C was chosen and incorporated into the thermal treatment for the freezing step of the lyophilisation cycle. This facilitated the fusion of smaller ice crystals together, to form larger crystals that leave large pores following ice sublimation[14].

The temperature selection for the freezing of the sample was to improve the homogeneity of crystallisation and formation of a porous ice cake [25]. Consequently, sponge-like, porous polymeric network of uniform and large pores that are regularly distributed throughout the

wafers were observed in figure 2 for POL-CAR-BLK-An and POL-SA-BLK-An wafers. The annealed wafers also had better elegance as compared to the non-annealed wafers. These wafers were deemed flexible enough to allow ease of handling for their application as an effective wound dressing with a low likelihood of causing contact irritation. To avoid collapse of the cake, primary drying of the sample was carried out at -25ºC at low pressure. Low chamber pressure allows for a high sublimation rate and homogenous heat transfer from the sample and for that purpose, chamber pressure was maintained between 20-50 mTorr.

The changes in the surface structure and reduced porosity of POL-CAR-DL-An wafers could be attributed to the different amounts of STP and DLF incorporated in the wafer's matrix. In terms of applications, the differences observed in the pore size morphologies of the POL-CAR-BLK An and NAn wafers can affect functional properties such as rate of hydration, swelling, adhesion and consequent drug release characteristics in the presence of wound exudate. Wafers with high porosity can absorb high exudate due to high water ingress which leads to high swelling and subsequent diffusion of drug from the swollen matrix[1,18]. Highly exuding chronic wounds such as diabetic foot and venous ulcers limit the application of dressings such as films due to the high amount of exudate which causes maceration at the wound site. Further, annealed POL-SA-DL-An wafers may offer a better drug delivery system due to their more porous nature compared to POL-CAR-DL-An wafer, and can therefore absorb high exudate volumes and also keep the wound environment moist for rapid healing. However, excessive hydration may cause wafer wetting and formation of slippery mucilage which can decrease the adhesion properties at the wound site[13,16].

For wound healing purposes, the freeze dried wafers are expected to encounter various stresses during its handling and application and therefore necessitates optimum mechanical strength, so as to maintain their structural integrity during and after application [26]. 'Hardness' is the measure of the peak force required to deform the wafer to the required depth of penetration. The

differences in hardness values observed between the POL-CAR and POL-SA wafers may be related to the different amounts of CAR and SA used in their respective formulations which may affect both how they interact with both POL and the loaded drug. Furthermore, the differences in the number, size and shape of pores between POL-CAR and POL-SA wafers could account for these differences in mechanical strength measured on the texture analyser[18].

The effect of speed and depth of compression on hardness are critical, as significant changes to wafer dimensions could affect properties such as its pore size[18]. Such variations if large enough (POL-CAR-BLK-NAn and POL-CAR-BLK-An) may result in significant changes in hydration, swelling and possibly drug release characteristics which ultimately affect its performance as a wound dressing for controlled drug delivery. However, this will need to be further investigated. Based on these results and the SEM observations, only annealed wafers were used for all subsequent investigations.

The crystalline properties of polymeric formulations affect various characteristics such as water uptake, bioadhesion and biodegradability of the polymers[27]. Wafers prepared from the POL-CAR and POL-SA showed decreased crystallisation of POL which may help to improve its properties stated above and therefore improve the performance of the dressing such as exudate absorption, prolonged retention at wound site which can ultimately increase the bioavailability of the drug and reduce the need for frequent change of dressing. The reduction in POL crystallization by SA and CAR is probably a result of interruption of POL-POL interactions because of formation of hydrogen bonds between the ether and hydroxyl groups from POL and SA or CAR respectively[28]. This decreased crystallanity of POL-CAR and POL-SA blends and the molecular dispersion of STP and DLF will have high surface energy due to less ordered amorphous structures than the more crystalline form. The increase in the surface energy allows greater molecular interaction between the solute and solvent hence they are more soluble and are expected to release the drugs (STP and DLF) quickly when applied to the wound site which can

help to reduce bacterial infection. However, it is important to maintain the amorphous form during storage since high energy levels in such form may cause a reversion back to the crystalline form of POL and DLF (which are respectively semi-crystalline and crystalline in nature) and needs further evaluation through long term stability studies.

However, Huang and co-workers reported that molecularly dispersed drug prompted by hydrogen bonding between drug and polymers had improved physical stability which did not affect release kinetics of the drug [29]. Such molecularly dispersed drug in the polymer matrix helps to improve physical stability and drug release from the dosage forms. This can help to maintain biological as well as environmental stability of STP and DLF and their expected controlled release will help to reduce the need for frequent dressing change dressing with improved wound healing [29].

The water uptake (swelling) of the samples reached the maximum value within 30 min of incubation, due to hydrophilicity of the POL, CAR and SA in the presence of SWF. In addition, the annealing process enhanced ice crystal size during the freezing stage and subsequently increase wafer porosity. The highly porous structure of freeze-dried wafers allowed a rapid ingress of water initially which affected the swelling capacity. It is interesting to note that the wafers maintained their structural integrity after 2 h of incubation at 37ºC due possibly to the mechanically stronger formulations obtained by annealing. This may be due to the effect of added drug which decreased the porosity (SEM data) as well as the formation of sodium sulphate which decreased the swelling capacity of wafers. Singh and co-workers reported the effect of sodium sulphate on gels of the polysaccharide, agarose. They showed that the hydration capacity of agarose polysaccharide decreased with increasing concentration of sodium sulphate which is associated with strong hydrophobic hydration of the highly osmotropic sodium sulphate [30]. The presence of sodium sulphate formed in the polymeric gels (POL-CAR and POL-SA) appears to be behaving in the same manner to reduce the swelling capacity of the DL wafers compared with

the BLK wafers. The mechanism behind this reduction is that a part of the total sodium sulphate present in the gel is used to reduce the interactions of hydrophilic -OH groups of CAR and SA with water molecules, thereby reducing the organization of water molecules into a tetrahedral arrangement in the vicinity of hydrated CAR and SA. The marked influence of sodium sulphate on the swelling index of POL-SA-DL-An and POL-CAR-DL-An may further affect the drug release through the wafers. Both (BLK and DL) wafers showed appropriate exudate holding capacity while maintaining their structural integrity for prolonged periods and therefore could help to overcome the challenge of excess exudate collecting under the dressing[1].

It is also possible that other factors apart from sodium sulphate maybe at play during hydration and swelling. For the systems containing SA (POL-SA-BLK and POL-SA-DL) the plateau regions of the swelling profiles could be due to the hydrogel formation caused by divalent calcium ions (Ca^{2+}) naturally present in alginates, which can exchange with sodium ions to form strong crosslinked hydrogels. In the case of systems containing CAR (POL-CAR-BLK and POL-CAR-DL) the decreasing trend of the profiles could be due to a partial solubilization of the systems which reduces their overall moisture holding capacity.

The adhesive characteristics showed differences between the BLK and DL wafers which again may be because of the presence of sodium sulphate in DL wafers which has a marked effect on the initial hydration of the wafers resulting in decreased stickiness. Cohesiveness is the intermolecular attraction which holds the wafer and the model wound substrate together. Usually thin watery serous type exudate (represented by 2% BSA SWF) in a wound signifies possible bacterial infection. *S. aureus* and *Streptococci* produce staphylokinase which has fibrinolytic activity and degrades fibrin clots resulting in thin watery exudate [31, 32]. The POL-CAR-DL-An and POL-SA-DL-An wafers can help to manage such exudate due to their porous nature. Haemorrhagic and haemopurulent (viscous and sticky) exudate signifies infection and trauma and POL-CAR (BLK-An and DL-An) wafers can provide prolonged retention of wafers at the

site of such wounds. Overall, adhesion results from both BLK-An and DL-An wafers confirmed that the porosity plays a critical role due to the ability to absorb SWF and hydration of the polymeric network (POL, SA and CAR). The decreased stickiness in the DL wafers was associated with the decreased porosity of these wafers due to the added drugs and subsequent sodium sulphate formation which inhibit rapid hydration of the wafers.

From the results obtained, it can be concluded that the wafers generally possessed good adhesive strength with the wound substrate containing two different types of exudate. Therefore these wafers are expected to adhere to the wound site and protect the wound from the external environment, with the absorption of large amounts of exudate, which is a primary requirement for a formulation to function as an ideal wound dressing. Generally, the force and work of adhesion values appear high and raises the issue of maintaining a balance between prolonged retention at the wound site and the need to avoid damaging sensitive newly formed tissue during the healing process in the course of dressing change. However, it should be noted that high adhesion will also reduce the need for frequent dressing changes and could therefore mitigate against damage to new tissues arising from high frequency of dressing changes. Further, normal moist dressings encounter a continuous flow of produced exudate which is expected to reduce the bioadhesion during the duration of application, compared to the current study where the volume of simulated fluid was kept constant. This however, requires further investigation during an *in vivo* study.

The rate of release was faster from the POL-CAR-DL-An wafers than the POL-SA-DL-An wafers within the first hour of release and attributed to the different ratios of POL, where POL-CAR wafer swelled more quickly and formed a gel that easily hydrated in the SWF during the initial stages of drug dissolution. Bunte and co-authors observed that drug release is facilitated by the porous network of lyophilised wafers[33]. An increased surface area of the dispersed drug in the porous cake occurs, accelerating dissolution significantly. The difference

in the drug released from both formulations may also be associated with the varying amount of STP and DLF present which can affect the drug release rate. As discussed previously in the swelling studies, POL-SA-DL wafers showed less swelling than the POL-CAR-DL-wafers which was also responsible for the slow release of STP. Both wafers showed very slow and constant release of DLF from the formulations with only 30-33% of DLF released from both wafers and might be attributed to its relatively poor water solubility as well as sodium sulphate which affected the hydration capacity of the wafers.

The slope (n) values from the Korsmeyer-Peppas equation, which characterises the release mechanism of drugs from cylindrical matrices (for wafers) can serve as an indication for diffusion controlled drug release, assuming wafer geometry with negligible edge effects, time- and position-independent diffusion coefficients in a non-swellable and insoluble matrix former. In contrast, if polymer swelling is the sole release rate controlling mechanism, zero order drug release kinetics are observed corresponding to a release exponent of n = 1. Release exponents that are in-between these extreme values for the respective device geometry indicate so-called anomalous or non-Fickian diffusion transport, with an overlapping of different types of phenomena, potentially including drug diffusion and polymer swelling [34]. Drug release from swellable matrices is usually complex and though some processes may be distinctly classified as either diffusion or erosion controlled, drug release is mostly governed by both mechanisms. Analysis of the experimental data using the Korsmeyer-Peppas equation, and interpretation of the release exponents (n), provides a better understanding of the mechanisms controlling release. Release exponents of POL-CAR-DL-An and POL-SA-DL-An wafers show an anomalous (non-Fickian) transport, suggesting that both diffusion of STP and DLF through the hydrated swollen polymer combined with gel erosion controlled drug release.

In the current study, the sterilization effect on the freeze-dried wafers was not investigated. However, the wafers will not be able to withstand heat or steam sterilization owing

to the potential to cause structural collapse due to moisture. The most suitable in our view will be gamma irradiation at a suitable dose. This was proved by Matthews and co-workers[16] who showed its suitability for sterilising freeze-dried polymeric wafers. At high doses, gamma rays were reported to cause a reduction in the rheological viscosity of the polymeric gels obtained from the wafers due possibly to breaking of hydrogen bonding. This will need further investigation in relation to the POL-CAR and POL-SA wafers used in this study.

5. Conclusions

Characterisation of the two different wafers (POL-CAR and POL-SA) (BLK-An and DL-An) showed significant differences in their microscopic structure and physical properties which is expected to impact on their wound healing performance characteristics. The annealing step in the lyophilisation cycle helped to produce soft, flexible and desired porous structure in the formulated wafers. This helped to improve mechanical strength, ease of hydration, adhesion and the *in vitro* drug release characteristics of the DL wafers. Further, the annealing step reduced the hardness of the wafers but remained strong enough to potentially withstand the mechanical stresses occurring during day-to-day activities, while flexible enough to prevent potential damage to newly formed skin tissue. DSC and XRD studies showed decreased crystallanity of the POL with molecular dispersion of the drugs within the wafer polymer matrix. Such dispersion of both drugs can improve the physical stability of the dosage form and controlled release of both drugs which can potentially help to improve wound healing by acting on two different stages of wound healing. The results show that the annealed wafers may be potentially used for highly exuding wounds such as chronic ulcers. However, this will need to be confirmed by further investigations in future *in vivo* animal studies.

6. References

1. Boateng JS, Matthews KH, Stevens HNE, Eccleston GM 2008. Wound healing dressings and drug delivery systems: A review. J Pharm Sci. 97(8):2892-2923.

2. Beldon P 2010. Basic science of wound healing. Surgery (Oxford) 28(9):409-412.

3. Enoch S, Leaper DJ 2008. Basic science of wound healing. Surgery (Oxford) 26(2):31-37.

4. Kirketerp-Moller K, Zulkowski K, James G 2011. Chronic Wound Colonization, Infection, and Biofilms. In Bjarnsholt T, Jensen PØ, Moser C, Høiby N, editors. Biofilm Infections, ed.: Springer New York. p 11-24.

5. Harding KG, Morris HL, Patel GK 2002. Science, medicine, and the future - Healing chronic wounds. Br. Med. J. 324 (7330):160-163.

6. Bryan J 2004. Moist wound healing: a concept that changed our practice. J Wound Care 13(6):227-8.

7. Menaker GM 2001. Wound dressings at the turn of the millennium. Curr. Probl. Dermatol. 13(2):86-89.

8. Adderley UJ 2010. Managing wound exudate and promoting healing. Br J Community Nurs. 15(3):S15-20.

9. Pielesz A, Machnicka A, E. S 2011. Antibacterial activity and scanning electron microscopy (SEM) examination of alginate-based films and wound dressings. Ecol. Chem. Eng. S 18(2):14.

10. Lloyd LL, Kennedy JF, Methacanon P, Paterson M, Knill CJ 1998. Carbohydrate polymers as wound management aids. Carbohydr. Polym. 37(3):315-322.

11. Sionkowska A 2011. Current research on the blends of natural and synthetic polymers as new biomaterials: Review. Prog. Polym. Sci. 36(9):1254-1276.

12. Pawar HV, Tetteh J, Boateng JS 2013. Preparation, optimisation and characterisation of novel wound healing film dressings loaded with streptomycin and diclofenac. Colloids Surf B Biointerfaces. 102:102-110.

13. Matthews KH, Stevens HNE, Auffret AD, Humphrey MJ, Eccleston GM 2005. Lyophilised wafers as a drug delivery system for wound healing containing methylcellulose as a viscosity modifier. Int. J. Pharm. 289(1-2):51-62.

14. Ayensu I, Mitchell JC, Boateng JS 2012. Development and physico-mechanical characterisation of lyophilised chitosan wafers as potential protein drug delivery systems via the buccal mucosa. Colloids Surf B Biointerfaces. 91:258-265.

15. Matthews KH, Stevens HNE, Auffret AD, Humphrey MJ, Eccleston GM 2008. Formulation, stability and thermal analysis of lyophilised wound healing wafers containing an insoluble MMP-3 inhibitor and a non-ionic surfactant. Int. J. Pharm. 356(1–2):110-120.

16. Matthews KH, Stevens HNE, Auffret AD, Humphrey MJ, Eccleston GM 2006. Gamma-irradiation of lyophilised wound healing wafers. Int. J. Pharm. 313(1-2):78-86.

17. Labovitiadi O, Lamb AJ, Matthews KH 2012. In vitro efficacy of antimicrobial wafers against methicillin-resistant Staphylococcus aureus. Ther. Delivery 3(4):443-455.

18. Boateng JS, Auffret AD, Matthews KH, Humphrey MJ, Stevens HNE, Eccleston GM 2010. Characterisation of freeze-dried wafers and solvent evaporated films as potential drug delivery systems to mucosal surfaces. Int. J. Pharm. 389(1–2):24-31.

19. Boateng JS, Pawar HV, Tetteh J 2013. Polyox and carrageenan based composite film dressing containing anti-microbial and anti-inflammatory drugs for effective wound healing. Int. J. Pharm. 441(1–2):181-191.

20. Lindsay S, DelBono M, Stevenson R, Stephens S, Breda C. 2010. The silver release profile of antimicrobial wound dressings: standardizing in vitro evaluations. (Poster) ed., USA.

21. Gethin, G 2007. The significance of surface pH in chronic wounds. Wounds UK, 3(3), 52-56

22. Prasad K, Kaneko Y, Kadokawa J 2009. Novel Gelling Systems of kappa-, iota- and lambda-Carrageenans and their Composite Gels with Cellulose Using Ionic Liquid. Macromol Biosci. 9(4):376-382.

23. Dalafu, H., Chua, M. T. and Chakraborty, S. (2010) 'Development of kappa-Carrageenan Poly (acrylic acid) Interpenetrating Network Hydrogel as Wound Dressing Patch', *Biomaterials*, 1054, 125-135.

24. Varshney, L. (2007) 'Role of natural polysaccharides in radiation formation of PVA-hydrogel wound dressing', *Nuclear Instruments & Methods in Physics Research Section B-Beam Interactions with Materials and Atoms,* 255(2), 343-349.

25. Tang X, Pikal M 2004. Design of Freeze-Drying Processes for Pharmaceuticals: Practical Advice. Pharm Res. 21(2):191-200.

26. Thakur RA, Florek CA, Kohn J, Michniak BB 2008. Electrospun nanofibrous polymeric scaffold with targeted drug release profiles for potential application as wound dressing. Int. J. Pharm. 364(1):87-93.

27. Prabaharan M, Gong S 2008. Novel thiolated carboxymethyl chitosan-g-beta-cyclodextrin as mucoadhesive hydrophobic drug delivery carriers. Carbohydr. Polym. 73(1):117-125.

28. Zivanovic S, Li J, Davidson PM, Kit K 2007. Physical, Mechanical, and Antibacterial Properties of Chitosan/PEO Blend Films. Biomacromolecules 8(5):1505-1510.

29. Huang J, Wigent RJ, Schwartz JB 2006. Nifedipine molecular dispersion in microparticles of ammonio methacrylate copolymer and ethylcellulose binary blends for controlled drug delivery: Effect of matrix composition. Drug Dev. Ind. Pharm. 32(10):1185-1197.

30. Singh T, Meena R, Kumar A 2009. Effect of sodium sulfate on the gelling behavior of agarose and water structure inside the gel networks. J. Phys. Chem. B 113(8):2519-2525.

31. White RJ, Cutting K, Kingsley A 2006. Topical antimicrobials in the control of wound bioburden. Ostomy Wound Manage 52(8):26-58.

32. Braff MH, Jones AL, Skerrett SJ, Rubens CE 2007. *Staphylococcus aureus* exploits cathelicidin antimicrobial peptides produced during early pneumonia to promote staphylokinase-dependent fibrinolysis. J. Infect. Dis. 195(9):1365-1372.

33. Bunte, H, Drooge, D J, Ottjes, G, Roukema, R, Verrijk, R, Yessine, M 2010. Key considerations when developing freeze-dried formulation and current trends', Pharmaceutical Technology Europe Digital, 22: 2-4.

34. Siepmann J, Siepmann F 2008. Mathematical modeling of drug delivery. Int. J. Pharm. 364(2):328-343.

Figure Legends

Figure 1: Schematic diagram of the lyophilisation cycle, incorporating an annealing step, used for the preparation of wafers.

Figure 2: SEM images of POL-CAR-BLK-NAn, POL-CAR-BLK-An, POL-CAR-DL-An, POL-SA-BLK-NAn, POL-SA-BLK-An, POL-SA-DL-An showing differences in porous microstructure due to annealing and presence of drug.

Figure 3: XRD diffractograms of pure polymers (SA, CAR and POL), drugs (STP and DLF) and POL-CAR and POL-SA (BLK and DL) wafers.

Figure 4: DSC profiles of the pure polymers, (SA, CAR and POL), drugs (STP and DLF) and POL-CAR and POL-SA (BLK-An and DL-An) wafers.

Figure 5: ATR-FTIR spectra showing peaks for different components within freeze dried POL-CAR and POL-SA (BLK-An and DL-An) wafers.

Figure 6: Swelling profiles (% swelling index against time) of POL-CAR and POL-SA wafers in the presence of normal SWF (mean ± SD, n=4).

Figure 7: Adhesion results showing the moist wound adhesion properties of POL-CAR and POL-SA wafers with SWF containing 2% w/w BSA and 5% w/w BSA.

Figure 8: *In vitro* drug release profiles of STP and DLF from POL-SA-DL-wafer and POL-CAR-DL-wafer showing plot of mean percent cumulative release (± SD, n=3) against time in the presence of SWF.

Table 1: Composition of polymers and drugs in gels used for freeze dried wafers. The final polymer concentration was 1 % w/w

Starting material	**POL-CAR-BLK**	**POL-CAR-DL**	**POL-SA-BLK**	**POL-SA-DL**
		Weight (g)		
POL	0.75	0.75	0.50	0.50
CAR	0.25	0.25	-	-
SA	-	-	0.50	0.50
STP	-	0.30	-	0.25
DLF	-	0.25	-	0.10
Total weight	1.00	1.55	1.00	1.35

Table 2: DSC of thermal transitions of the POL-CAR and POL-SA gels (NAn and An) frozen to -60°C and then reheated to and held at -25°C. The results show no transitions around -25°C

Samples (gels)	Temperature (°C)							
	Glass transition		Eutectic melt			Ice melt		
	Onset	Midpoint	Onset	Peak	Endset	Onset	Peak	Endset
POL-CAR	-55.8	-54.5	-12.4	-10.1	-8.5	-0.4	3.0	7.3
POL-CAR-An	-	-	-13.5	-10.5	-8.65	-0.9	2.0	6.8
POL-SA	-58.3	-56.9	-11.6	-9.7	-8.2	-0.8	3.5	8.9
POL-SA-An	-	-	-11.2	-9.5	-8.3	-1.0	2.6	11.1

Table 3: Texture analysis data showing changes in mechanical resistance of the various wafers with different formulation and instrumental variables (speed of compression, depth of penetration and annealing during freeze-drying

			Force (N)			
Speed (mm/s)	**POL-CAR-BLK (NAn)**	**POL-CAR-BLK (An)**	**POL-CAR-DL (An)**	**POL-SA-BLK (NAn)**	**POL-SA-BLK (An)**	**POL-SA-DL (An)**
n = 5	**Mean ± SD**	**Mean ± SD**	**Mean ± SD**	**Mean ± SD**	**Mean ± SD**	**Mean ± SD**
0.2	1.62 ± 0.2	0.91 ± 0.1	0.63 ± 0.0	0.47 ± 0.1	0.27 ± 0.1	0.38 ± 0.1
0.5	1.72 ± 0.1	0.96 ± 0.3	0.69 ± 0.1	0.51 ± 0.1	0.34 ± 0.1	0.47 ± 0.1
1.0	1.82 ± 0.1	0.97 ± 0.2	0.71 ± 0.1	0.63 ± 0.1	0.29 ± 0.1	0.51 ± 0.1
2.0	1.96 ± 0.4	0.96 ± 0.1	0.77 ± 0.0	0.50 ± 0.1	0.44 ± 0.1	0.55 ± 0.1
3.0	2.16 ± 0.1	1.31 ± 0.3	0.72 ± 0.1	0.63 ± 0.1	0.46 ± 0.1	0.58 ± 0.1
Depth (mm)	**POL-CAR-BLK (NAn)**	**POL-CAR-BLK (An)**	**POL-CAR-DL (An)**	**POL-SA-BLK (NAn)**	**POL-SA-BLK (An)**	**POL-SA-DL (An)**
n = 5	**Mean ± SD**	**Mean ± SD**	**Mean ± SD**	**Mean ± SD**	**Mean ± SD**	**Mean ± SD**
0.2	0.75 ± 0.2	0.04 ± 0.0	0.06 ± 0.0	0.03 ± 0.0	0.02 ± 0.0	0.04 ± 0.0
0.5	0.92 ± 0.2	0.14 ± 0.0	0.20 ± 0.1	0.23 ± 0.1	0.06 ± 0.0	0.08 ± 0.0
1.0	1.24 ± 0.2	0.45 ± 0.1	0.38 ± 0.1	0.34 ± 0.1	0.17 ± 0.0	0.18 ± 0.1
1.5	1.57 ± 0.2	0.77 ± 0.1	0.54 ± 0.0	0.51 ± 0.1	0.23 ± 0.1	0.37 ± 0.1
2.0	1.57 ± 0.2	0.96 ± 0.1	0.66 ± 0.0	0.50 ± 0.1	0.35 ± 0.1	0.51 ± 0.2
3.0	1.80 ± 0.3	1.19 ± 0.3	0.90 ± 0.0	0.80 ± 0.1	0.54 ± 0.1	0.66 ± 0.2
'Hardness'	**POL-CAR-BLK (NAn)**	**POL-CAR-BLK (An)**	**POL-CAR-DL (An)**	**POL-SA-BLK (NAn)**	**POL-SA-BLK (An)**	**POL-SA-DL (An)**
n = 4	**Mean ± SD**	**Mean ± SD**	**Mean ± SD**	**Mean ± SD**	**Mean ± SD**	**Mean ± SD**
(N)	1.06 ± 0.4	0.96 ± 0.1	0.74 ± 0.3	0.50 ± 0.1	0.44 ± 0.1	0.55 ± 0.1

Table 4: Release parameters obtained from fitting experimental drug dissolution (release) data to different kinetic equations for wafers containing STP and DLF.

Formulation	Zero order		First order		Higuchi		Hixon Crowell		Korsmeyer-Peppas		
	K_0	R^2	K_1	R^2	K_H (% $min^{1/2}$)	R^2	K_{HC} (% $min^{-1/3}$)	R^2	K_P (% min^{-n})	n	R^2
STP											
POL-CAR-DL-An	0.28	0.58	0.004	0.97	4.260	0.97	-0.005	0.95	0.400	0.60	0.95
POL-SA-DL-An	0.20	0.54	0.001	0.95	3.010	0.97	-0.003	0.93	0.320	0.57	0.97
DLF											
POL-CAR-DL-An	0.28	0.58	0.004	0.97	4.260	0.97	-0.005	0.95	0.400	0.60	0.95
POL-CAR-DL-An	0.28	0.58	0.004	0.97	4.260	0.97	-0.005	0.95	0.400	0.60	0.95

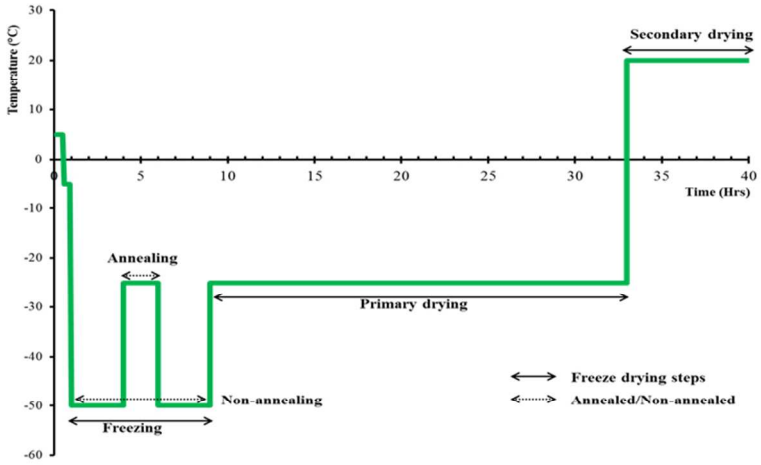

254x190mm (96 x 96 DPI)

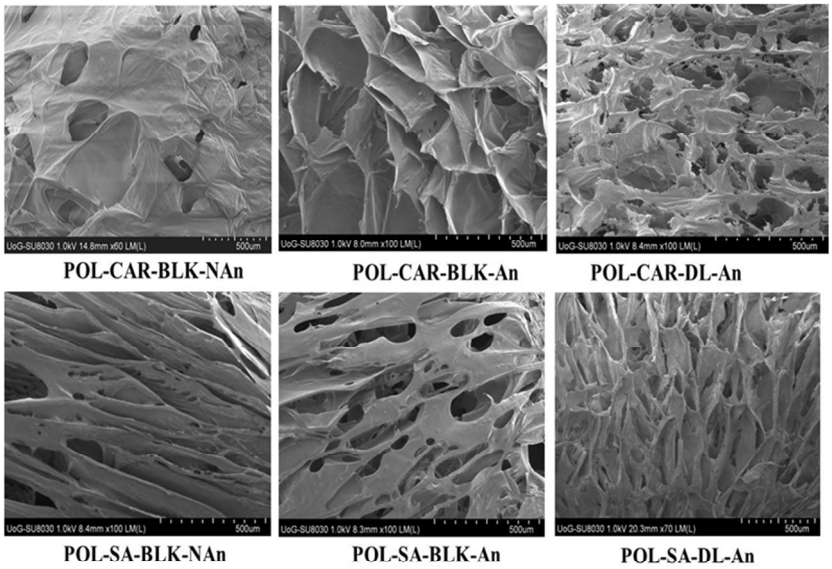

Figure 2
254x190mm (96 x 96 DPI)

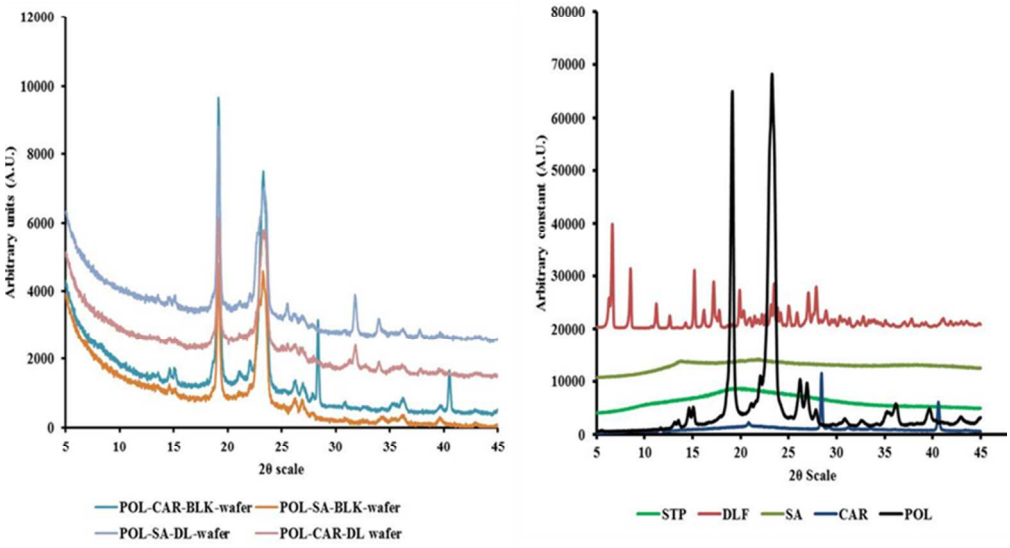

Figure 3
254x190mm (96 x 96 DPI)

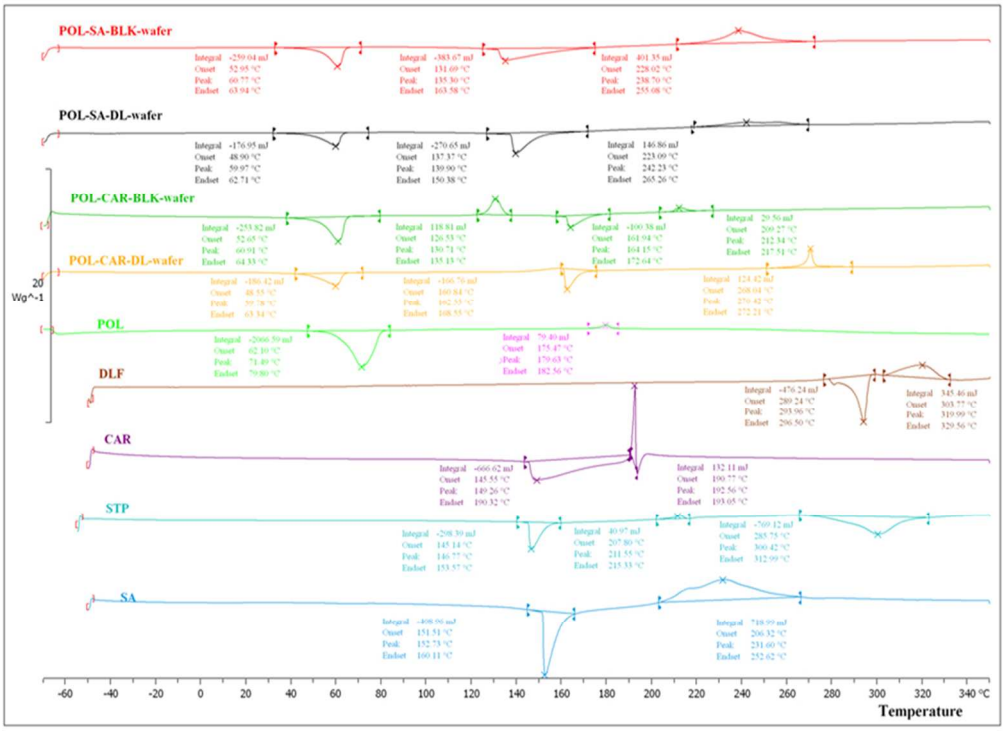

Figure 4
254x190mm (96 x 96 DPI)

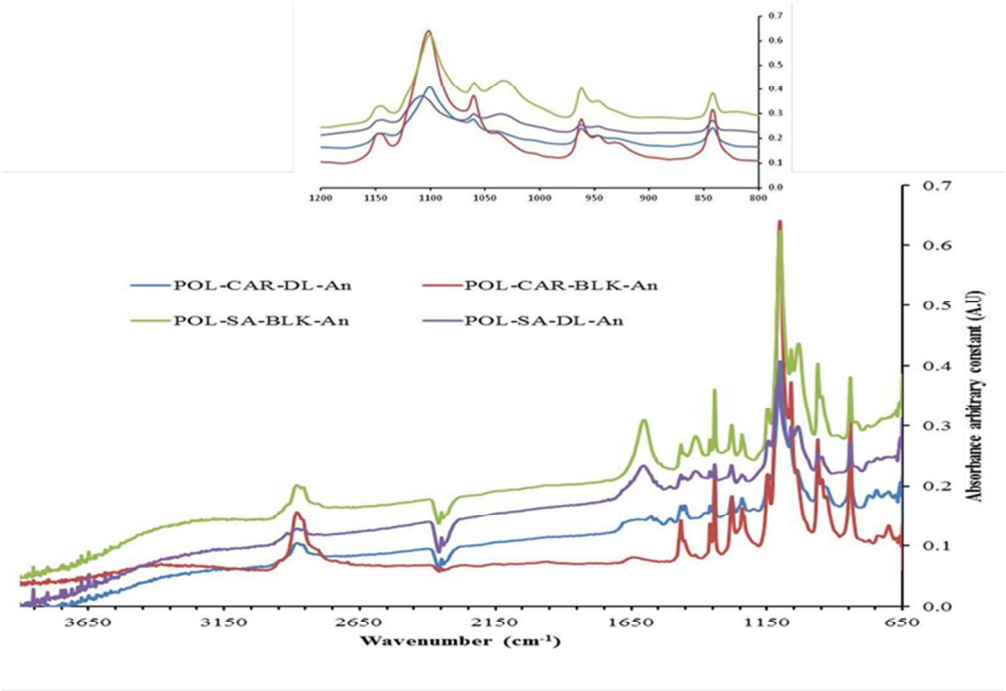

Figure 5
254x190mm (96 x 96 DPI)

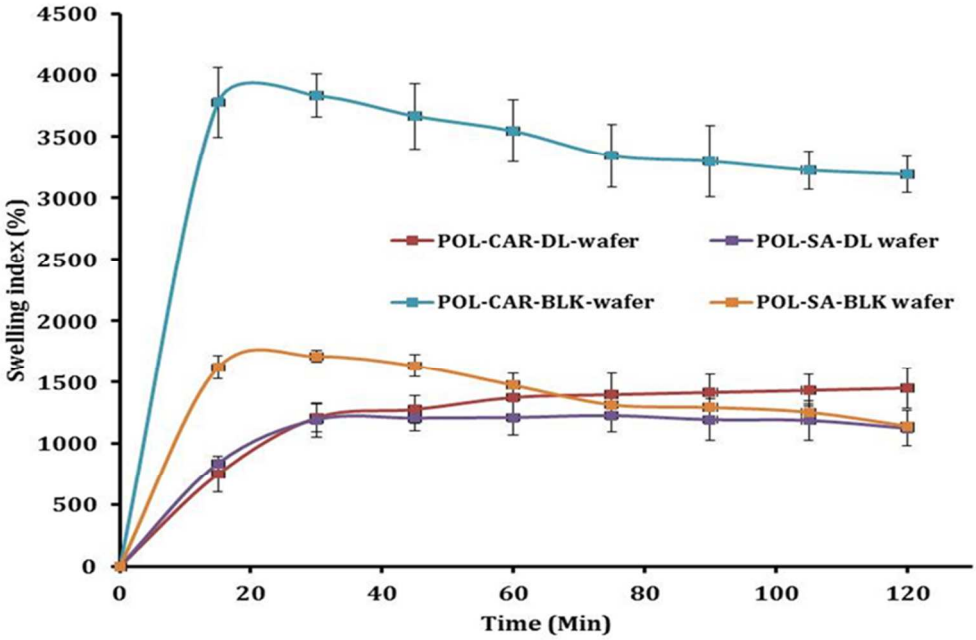

254x190mm (96 x 96 DPI)

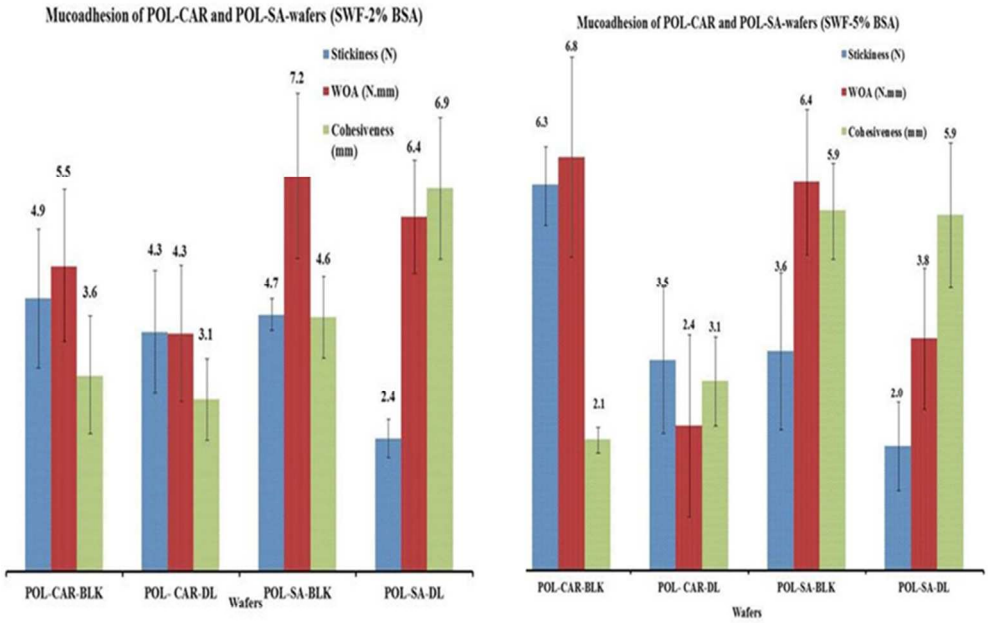

254x190mm (96 x 96 DPI)

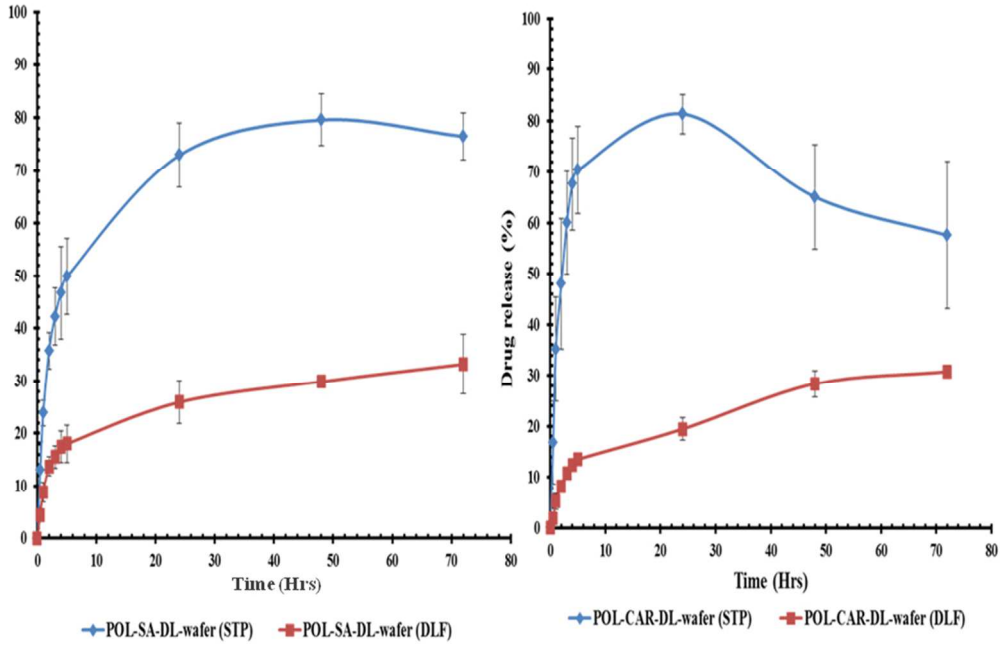

254x190mm (96 x 96 DPI)